Biophysical Journal Volume 76 May 1999 2861–2867

Cyclic AMP Diffusion Coefficient in Frog Olfactory Cilia

Chunhe Chen,* Tadashi Nakamura,# and Yiannis Koutalos*

*Department of Physiology and Biophysics, University of Colorado Health Sciences Center, Denver, Colorado 80262 USA, and #Department of Applied Physics and Chemistry, The University of Electrocommunications, Chofu, Tokyo 182-8585, Japan

ABSTRACT Cyclic AMP (cAMP) is one of the intracellular messengers that mediate odorant signal transduction in vertebrate olfactory cilia. Therefore, the diffusion coefficient of cAMP in olfactory cilia is an important factor in the transduction of the odorous signal. We have employed the excised cilium preparation from the grass frog (*Rana pipiens*) to measure the cAMP diffusion coefficient. In this preparation an olfactory cilium is drawn into a patch pipette and a gigaseal is formed at the base of the cilium. Subsequently the cilium is excised, allowing bath cAMP to diffuse into the cilium and activate the cyclic nucleotide-gated channels on the plasma membrane. In order to estimate the cAMP diffusion coefficient, we analyzed the kinetics of the currents elicited by step changes in the bath cAMP concentration in the absence of cAMP hydrolysis. Under such conditions, the kinetics of the cAMP-activated currents has a simple dependence on the diffusion coefficient. From the analysis we have obtained a cAMP diffusion coefficient of $2.7 \pm 0.2 \cdot 10^{-6}$ cm^2 s^{-1} for frog olfactory cilia. This value is similar to the expected value in aqueous solution, suggesting that there are no significant diffusional barriers inside olfactory cilia. At cAMP concentrations higher than 5 μM, diffusion slowed considerably, suggesting the presence of buffering by immobile cAMP binding sites. A plausible physiological function of such buffering sites would be to prolong the response of the cell to strong stimuli.

INTRODUCTION

The first steps in the detection of odorous substances by vertebrates take place in the olfactory receptor neurons of the nasal neuroepithelium. Odorous stimuli trigger a sequence of events leading to membrane depolarization and discharge of action potentials that transmit the information to the brain. The olfactory receptor neuron is bipolar, the one end extending dendrites to the surface of the neuroepithelium and the other end sending axons that terminate in the olfactory bulb in the brain. The dendrites form knobs from which specialized cilia emanate, where the initial steps of olfactory signal transduction take place (for reviews of olfactory transduction see Ronnett and Snyder, 1992; Breer et al., 1994; Schild and Restrepo, 1998). Cyclic AMP (cAMP) is one of the intracellular messengers involved in olfactory signal transduction. cAMP is synthesized by an adenylate cyclase and hydrolyzed by a phosphodiesterase. Odorant molecules bind to and activate receptor proteins located on the membrane of the cilia. The activated receptors stimulate an olfactory specific G-protein, G_{olf} (Pace and Lancet, 1986; Jones and Reed, 1989; Firestein et al., 1991), which, in turn, enhances the synthesis of cAMP by the adenylate cyclase (Pace et al., 1985; Sklar et al., 1986; Bakalyar and Reed, 1990), leading to an increase in the cAMP concentration. cAMP binds to and opens cyclic nucleotide-gated channels located on the ciliary plasma membrane (Nakamura and Gold, 1987), allowing the influx of Na^+ and Ca^{2+}, thereby depolarizing the cell membrane and generating action potentials. The influx of Ca^{2+} through the cyclic nucleotide-gated channels serves to amplify the response by activating a chloride current (Kleene and Gesteland, 1991b; Kleene, 1993; Kurahashi and Yau, 1993; Dubin and Dionne, 1994). Ca^{2+} is also involved in the recovery process and in adaptation by reducing the apparent affinity of the cyclic nucleotide-gated channels for cAMP (Kramer and Siegelbaum, 1992; Chen and Yau, 1994; Kurahashi and Menini, 1997) and perhaps by stimulating the hydrolysis of cAMP by the phosphodiesterase (Borisy et al., 1992). In addition to cAMP, other transmitters may also be involved in olfactory transduction. Several odorants have been shown to stimulate the production of IP_3 (Breer et al., 1990; Ronnett et al., 1993), resulting in the influx of Ca^{2+} through IP_3-gated channels (Restrepo et al., 1990; Cunningham et al., 1993). Ca^{2+} can then affect several processes, resulting in membrane depolarization. Other pathways may involve cyclic GMP (cGMP), which can also open the ciliary membrane cyclic nucleotide-gated channels. cGMP is proposed to be synthesized by a guanylate cyclase, which in this case can be activated by nitric oxide or carbon monoxide (Verma et al., 1993; Breer and Shepherd, 1993).

With regard to the cAMP-mediated aspects of olfactory signal transduction, the amplitude, as well as the kinetics of the response to odorant stimulation, will also depend on the spread of activation of the cyclic nucleotide-gated channels along the length of the cilium. Since the spread of activation depends on the diffusion coefficient of cAMP, the latter is an important factor in the shaping of the response of the olfactory receptor neuron. There is evidence, based on whole cell responses elicited by the photolysis of caged cAMP (Lowe and Gold, 1993), suggesting that the value of the cAMP diffusion coefficient in cilia cannot be much

Received for publication 4 December 1998 and in final form 27 January 1999.

Address reprint requests to Dr. Yiannis Koutalos, University of Colorado Health Sciences Center, Department of Physiology and Biophysics, Box C-240, 4200 East Ninth Avenue, Denver, CO 80262. Tel.: 303-315-4418; Fax: 303-315-8110; E-mail: yiannis.koutalos@uchsc.edu.

0006-3495/99/05/2861/07 $2.00

lower than the value in solution. In this study we present direct measurements of the cAMP diffusion coefficient in cilia, based on a method developed by Koutalos et al. (1995a) for rod photoreceptor outer segments. We have dialyzed cAMP into excised cilia, while using the cyclic nucleotide-gated channels on the membrane of the cilium to monitor the internal cAMP concentration. We could determine the cAMP diffusion coefficient from the kinetics of the currents elicited by step changes in the bath cAMP concentration. At low cAMP concentrations, the value of the cAMP diffusion coefficient we measured is similar to the value in solution. At concentrations >5 μM, the value of the apparent diffusion coefficient is reduced because of buffering.

MATERIALS AND METHODS

Grass frogs (*Rana pipiens*) (Blue Spruce, Castlerock, CO) were decapitated and pithed. The olfactory epithelia were dissected and olfactory receptor neurons were isolated according to the method of Nakamura et al. (1996). In this cell preparation the cilia do not move very fast, permitting the measurement of their length through the microscope before excision.

Patch pipettes were made from thin-walled borosilicate glass (World Precision Instruments, Sarasota, FL) using a Sutter P-97 horizontal puller. The pipettes were fire-polished to a small diameter with the puller and the bubble number was checked for each pipette. Only pipettes with bubble numbers between 2.5 and 3.5 (empty pipette resistance ~30 MΩ) were used for recording. Currents were recorded under voltage clamp from excised cilia using a List EPC-7 amplifier and Axoscope software (Axon Instruments, Foster City, CA). A single cilium was drawn into a patch pipette and a high-resistance seal (>1 GΩ) was formed at the base of the cilium (Kleene and Gesteland, 1991a; Nakamura et al., 1996). The cilium was then excised from the cell by gently tapping the micromanipulator. The excised cilium allowed the simultaneous dialysis of the intracellular space and recording of the ciliary membrane current through the patch pipette. The membrane potential was held at −40 mV throughout the experiment unless stated otherwise. In all of the experiments the patch pipette contained a simplified saline solution (in mM: 120 NaCl, 5 HEPES, pH 7.20). The bath solution was based on the simplified saline and contained (in mM): 120 NaCl, 5 HEPES, 0.2 EGTA, 0.2 EDTA, pH 7.20. The bath solution also contained 0.5 mM 3-isobutyl-1-methylxanthine (IBMX) and different concentrations of cAMP. The IBMX was used in order to inhibit any phosphodiesterase activity present in the cilia. In some experiments IBMX was omitted, so that the effect of the phosphodiesterase activity on the current kinetics could be observed. Since neither the pipette nor the bath solution contained Ca^{2+}, the Ca^{2+}-activated Cl^- channels (Kleene and Gesteland, 1991b; Kleene, 1993; Kurahashi and Yau, 1993) do not contribute to the observed currents; the observed currents are carried by Na^+, flowing through the cyclic nucleotide-gated channels. Changes of bath solution were performed using a fast perfusion system (SF-77B, Warner Instruments, Hamden, CT). Solution changes around the pipette tip were complete within 20 ms as judged from junction currents (data not shown).

All reagents were of analytical grade. The experiments were carried out at room temperature. Electrical records were low-pass filtered at 20 Hz and digitized at 100 Hz. In all of the figures, inward membrane current is plotted as a negative current.

Data analysis

Frog olfactory cilia have a diameter of 0.2–0.3 μm (Menco, 1980). The much smaller diameter of the cilia compared to their length (25–46 μm in this study) allows us to assume that the diffusion of cAMP is essentially taking place in one dimension along the length of the cilium. Then, in the absence of cAMP hydrolysis, the concentration $C(x, t)$ of cAMP inside the cilium at distance x from the closed end of the cilium and time t satisfies the diffusion equation:

$$\frac{\partial C(x, t)}{\partial t} = D \cdot \frac{\partial^2 C(x, t)}{\partial x^2} \tag{1}$$

where D is the diffusion coefficient. Equation 1 assumes that the movement of cAMP, which is negatively charged, does not depend on the electric field between the pipette and bath electrodes. The validity of this assumption was corroborated experimentally (see Results). Since the bath solution change took much less time to complete (20 ms, see Materials and Methods) than the time required for cAMP to reach equilibrium within the cilium (>1 s, see Results), the change in cAMP concentration at the open end of the cilium can be considered to be instantaneous. This allows us to solve Eq. 1 according to the method presented in Koutalos et al. (1995a).

We introduce the dimensionless variables X and T:

$$X = x/L \tag{2}$$

$$T = Dt/L^2 \tag{3}$$

where L is the length of the cilium. Then, the concentration of cAMP inside the cilium can be evaluated for the situation when the cAMP concentration is switched on at the open end of the cilium and for the situation when the cAMP is removed from the open end. It can be evaluated as a function $C(X, T)$ of X and T, according to Eqs. 8a and 8b in Koutalos et al. (1995a). The advantage of introducing the dimensionless variables is that the cAMP concentration as evaluated by $C(X, T)$ is independent of the value of the diffusion coefficient and the length of the cilium.

When cAMP has reached equilibrium inside the cilium, we can relate the cAMP concentration, C, to the ciliary current, J, in terms of the Hill equation:

$$J = J_{\max} \cdot \frac{C^n}{C^n + K_{1/2}^n} \tag{4}$$

where $J_{\max}$ is the saturated current elicited with 20 μM cAMP (see Nakamura and Gold, 1987), and $K_{1/2}$ and n are the half-activating cAMP concentration and the Hill coefficient, respectively.

The enzymatic machinery of olfactory transduction, including the cyclic nucleotide-gated channels, is equidistributed along the length of the cilium (Lowe and Gold, 1991). Also, since the interaction of cAMP with the channel takes place in the order of milliseconds (Lowe and Gold, 1993), the current kinetics reflect the kinetics of diffusion rather than the kinetics of the interaction between cAMP and channel. Therefore, for the time-dependence of the current recorded by the patch pipette we can write

$$J(T) = J_{\max} \cdot \int_0^1 \frac{C^n(X, T)}{C^n(X, T) + K_{1/2}^n} \cdot dX. \tag{5}$$

$J(T)$ can be evaluated for each excised cilium and fitted to the observed current time course obtained upon changing bath cAMP. For fitting, the template $J(T)$ is scaled on the time axis to match the experimental record in real time, $J(t)$:

$$J(t) = J(T/\alpha) \tag{6}$$

where α is the scaling factor. This approach was valid for low cAMP concentrations, for which there was no significant buffering and both the rising and falling phases could be described with a single diffusion coefficient. Slight deviations of the theoretical fits from the experimental records were observed (Fig. 3), probably reflecting the slight divergence of the actual cilium from the idealized type used to develop the diffusion model. More specifically, the distribution of the cyclic nucleotide-gated channels along the length of the cilium is unlikely to be perfectly homogeneous, while the cilium, having a taper, is not a perfect cylinder either.

Space-clamp failure may also contribute to the observed discrepancies between the shapes of the theoretical templates and the experimental records (see below). Similar deviations between theoretical templates and experimental records have also been observed in rod photoreceptors (Koutalos et al., 1995a, Figs. 5 and 6).

At higher cAMP concentrations, the rising phase was sometimes biphasic, indicating the presence of significant buffering. In such cases, Eq. 6 was used to fit the early part of the rising phase, a procedure that would give the diffusion coefficient at low cAMP concentrations, i.e., in the absence of buffering. The analysis of the falling phase in the presence of significant buffering was based on the exponential relaxation of the latter part of the current upon removal of cAMP. In this case the rate of decay is given by $\pi^2 \cdot n \cdot \alpha/4$ (Koutalos et al., 1995b), allowing the determination of α.

Since, from Eq. 3:

$$\alpha = D/L^2 \tag{7}$$

D can be obtained from collected results as the slope of the plot of α versus $1/L^2$.

One concern with the experiments described here is the possibility of a space-clamp failure that would diminish current collection from the distal part of the cilium. For the lengths of the cilia employed in these experiments (25–46 μm) space-clamp problems might lead to an underestimation of the current by 20–30% (Lowe and Gold, 1993; Kleene et al., 1994). Because, as argued in Koutalos et al. (1995a), the current kinetics depend mostly on the kinetics of cAMP diffusion, such current underestimations should not have a significant effect on the measured value of the diffusion coefficient. A related concern is whether the full length of the cilium is accessible to cAMP diffusion. The presence of occlusions along the length of the cilium would diminish the effective length and result in an overestimation of the diffusion coefficient. Such occlusions are rather unlikely since the values of the kinetic parameter α are found to be proportional to $1/L^2$ (see Results). The presence of occlusions would have resulted in values of α that would vary randomly with length L.

RESULTS AND DISCUSSION

Fig. 1 shows membrane current recordings from an excised frog olfactory cilium. The length of the cilium, L, was 38 μm. The membrane potential was V = −40 mV. Inward membrane currents, carried by Na^+, were elicited by step changes of cAMP in the bath. The bath solution contained IBMX as well. The saturated current, J_{max}, was ~180 pA.

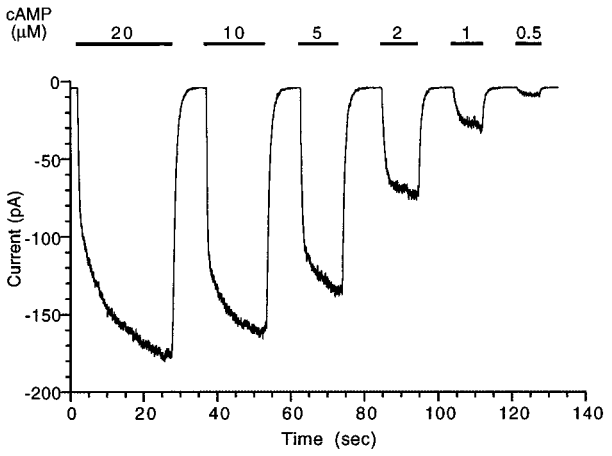

FIGURE 1 Currents elicited by different concentrations of cAMP from an excised olfactory cilium. L = 38 μm; V = −40 mV.

The value of J_{max} varied from ~40 to ~210 pA among different cilia, but did not correlate with the length of the excised cilium. Although we do not know the reasons for this variability, it might reflect differences in the number of cyclic nucleotide-gated channels originally present in the cilium. Fig. 2 *A* shows the relationship between the steady-state current and cAMP concentration for the cilium of Fig. 1. The data were fitted with Eq. 4 (*smooth curve*), giving a half-activation constant, $K_{1/2}$, of 2.8 μM and a Hill coefficient, n, of 1.8. Averaged data from six cilia are shown in Fig. 2 *B*. The Hill equation fit gave values $K_{1/2}$ = 3.3 μM and n = 1.8. These values are in good agreement with results obtained from excised patches (Nakamura and Gold, 1987; Frings et al., 1992; for reviews see Zufall et al., 1994; Finn et al., 1996).

For the cilium of Fig. 1, templates $J(T)$ were constructed for the rising and falling phases of the cAMP-induced currents according to Eq. 5 and the specified values of $K_{1/2}$,

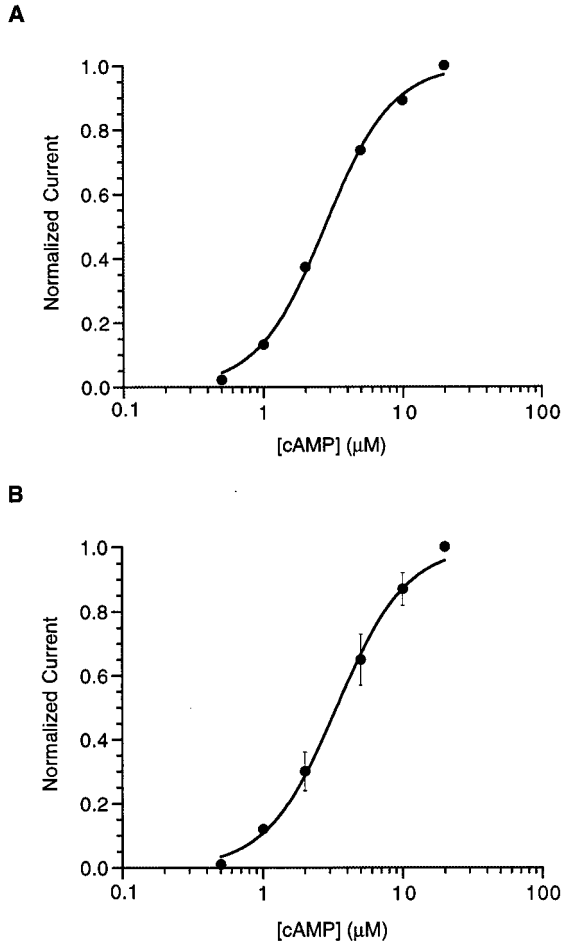

FIGURE 2 Dependence of steady-state currents on cAMP concentration. (*A*) Steady-state currents plotted as a function of the cAMP concentration for the experiment of Fig. 1. The currents have been normalized with respect to the current at 20 μM cAMP. The smooth curve is the Hill equation (Eq. 4) with $K_{1/2}$ = 2.8 μM and n = 1.8. (*B*) Averaged results from six cilia. Error bars indicate standard errors. The smooth curve is a least-squares fit according to the Hill equation, giving $K_{1/2}$ = 3.3 μM and n = 1.8.

n, and J_{max}. These templates were scaled according to Eq. 6 so that they fitted the rising and the falling phases of the currents shown in Fig. 1. Fig. 3 *A* shows the fits for the current elicited by 0.5 μM cAMP. The scaling factor, α, was 0.25 s^{-1} and 0.30 s^{-1} for the rising and the falling phase, respectively. Fig. 3, *B* and *C* show similar fittings for exposures to cAMP concentrations of 1 and 2 μM. At these low cAMP concentrations, the rising and the falling phases of the currents could be described by a single diffusion coefficient. In all three panels, systematic differences between the shapes of the theoretical templates and the shapes of the experimental records are evident. Such differences were observed in virtually all examined cilia, and, as discussed in the section on Data Analysis, they probably reflect slight deviations from the assumptions used to develop the theoretical model.

For the currents shown in Fig. 1, and at cAMP concentrations >5 μM, a secondary, slow rise was evident after the early rapid rise of the current activated by cAMP. This secondary phase became more prominent at higher cAMP concentrations and is likely to be due to buffering by immobile cAMP binding sites. Such sites would reversibly bind cAMP and slow its diffusion at concentrations higher than 5 μM. This would suggest that the affinity of the binding sites for cAMP should be higher than at least 5 μM. Fig. 4 *A* shows the current elicited by 5 μM in Fig. 1. The solid line represents a $J(T)$ template, fitted to the early part of the rising phase, giving a scaling factor of 0.30 s^{-1}. The latter part of the rising phase is significantly slower and cannot be adequately described by the same scaling factor. The latter part of the falling phase was fitted with an exponential curve (*dashed line*) with a decay rate of 1.06 s^{-1}, giving a scaling factor of 0.24 s^{-1}. The currents elicited by 10 and 20 μM cAMP (Fig. 4, *B* and *C*, respectively) were analyzed in the same way. Although the rising phase of the current was significantly slowed by buffering, no slowing was generally evident in the falling phase of the current

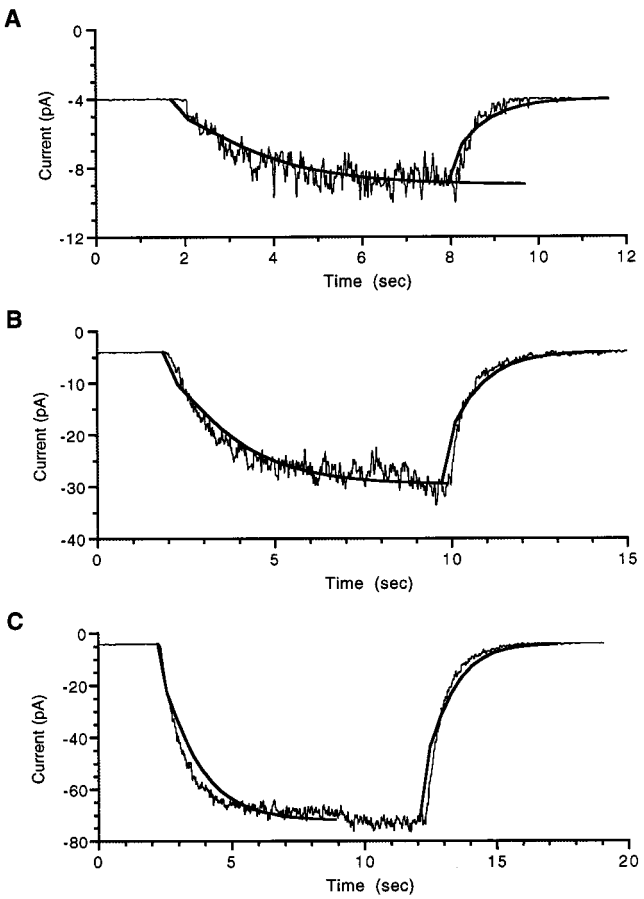

FIGURE 3 Determinations of the scaling factor α from currents activated by low concentrations of cAMP. (*A*) Scaled fits of the template $J(T)$ (*thick lines*) to the current record (*thin line*) for the 0.5 μM cAMP step in Fig. 1. The scaling factor α was 0.25 s^{-1} and 0.30 s^{-1} for the rising and the falling phase, respectively. (*B*) Template fits for the 1 μM cAMP step in Fig. 1. α = 0.25 s^{-1} for both the rising and falling phases. (*C*) Template fits for the 2 μM cAMP step in Fig. 1. α = 0.30 s^{-1} for the rising phase and 0.25 s^{-1} for the falling phase.

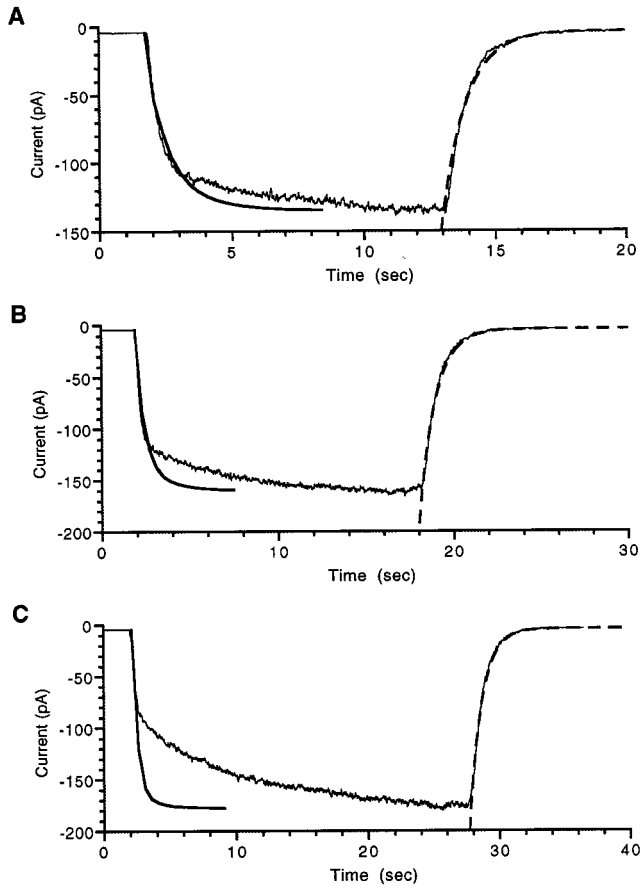

FIGURE 4 Determinations of the scaling factor α from currents activated by high concentrations of cAMP. (*A*) The solid line is a scaled fit of the template $J(T)$ to the early rising phase of the current elicited by the 5 μM cAMP step in Fig. 1. The scaling factor α was 0.30 s^{-1}. The dashed line is an exponential fit to the falling phase, giving a scaling factor of 0.23 s^{-1}. (*B*) Analysis of the current elicited by 10 μM cAMP in Fig. 1. The scaling factors for the rising and the falling phase were 0.25 s^{-1} and 0.24 s^{-1}, respectively. (*C*) Analysis of the current elicited by 20 μM cAMP in Fig. 1. The scaling factors for the rising and the falling phase were 0.20 s^{-1} and 0.23 s^{-1}, respectively.

upon removal of cAMP. This asymmetric effect of buffering is perhaps indicative of a slow buffer that is acting like a sink for cAMP. Unfortunately, because of the saturation of the cyclic nucleotide-gated channels at the higher cAMP concentrations, the properties of the buffer could not be analyzed in greater detail.

For the cilium of Fig. 1, the average scaling factor from a total of 12 determinations was $\alpha = 0.25 \pm 0.01\ s^{-1}$ (mean ± SEM). For a length $L = 38\ \mu m$, this value of α gives a diffusion coefficient $D = 3.7 \pm 0.1 \cdot 10^{-6}\ cm^2\ s^{-1}$ (mean ± SEM) for low cAMP concentrations (<5 μM). cAMP-activated currents from other cilia were analyzed in the same fashion. When there was no indication of buffering, the scaling factors were obtained as in Fig. 3, by fitting the overall time course of the rising or falling phase. When there was an indication of buffering, the currents were analyzed as in Fig. 4, by fitting the early part of the rising phase with the appropriate template and by obtaining the relaxation rate of the falling phase.

Under the experimental conditions, cAMP is negatively charged. It is conceivable that the electric field between the pipette and bath electrodes used to set the membrane voltage affects the movement of cAMP. We have examined this possibility by measuring the cAMP diffusion coefficient at different membrane voltages. Fig. 5 *A* shows the currents (corrected for leak) activated by steps of 20 μM cAMP at different membrane potentials. The currents were normalized over their maximum value and plotted on a logarithmic scale in Fig. 5 *B*. The decays of the currents upon removal of cAMP were exponential. In a semilogarithmic scale, these decays comprised a set of virtually parallel straight lines, indicating that the decay rate was independent of voltage. Subsequently, for each voltage, the diffusion coefficient was calculated from the decay rate. Fig. 6 graphically shows the independence of the diffusion coefficient from membrane voltage.

The scaling factors for the rising and falling phases of a current activated by a particular cAMP concentration were usually not identical. Nevertheless, the difference between the two factors was not systematic across cilia or cAMP concentrations. The presence of an appreciable hydrolytic activity would have resulted in significantly slower kinetics for the rising phase compared to the falling phase. Fig. 7 shows the currents activated by 5 μM cAMP in the *presence* of 0.5 mM IBMX and by 200 μM cAMP in the *absence* of IBMX for a cilium of length $L = 46\ \mu m$. As expected, the phosphodiesterase activity markedly slows the rising phase and speeds the decay of the current. For the cAMP-activated current in the presence of IBMX, the scaling factors were 0.07 and 0.10 s^{-1} for the rising and the falling phase, respectively. For the cAMP-activated current in the absence of IBMX, the scaling factors were 0.008 and 1.12 s^{-1} for the rising and the falling phase, respectively, with a ratio of 140. The absence of any systematic difference between the rising and falling phase kinetics in the presence of 0.5 mM IBMX indicates that this concentration of IBMX was adequate for abolishing any significant hydrolytic activity inside the cilia. It is interesting to note that for this cilium, the kinetics of the current elicited by 5 μM cAMP show no evidence of buffering. Compared to the cilium of Fig. 1, the lack of buffering at this concentration could be the result of a lower concentration of cAMP binding sites for this cilium, or a lower affinity of these sites for cAMP.

Fig. 8 shows the collected results for the scaling factors obtained from seven cilia. The straight line is a least-squares fit through the data, constrained to pass through the origin.

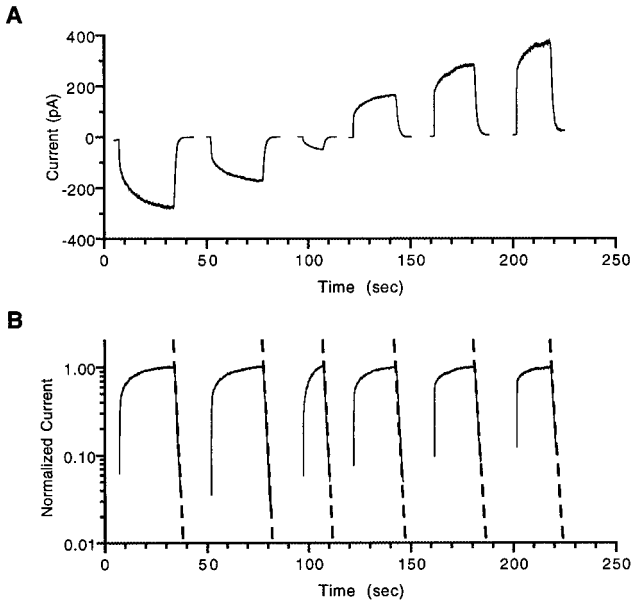

FIGURE 5 Dependence of the amplitude and kinetics of the cAMP-activated current on membrane voltage. (*A*) Currents elicited by 20 μM cAMP at different voltages. Leak currents have been subtracted. From left to right, membrane voltage was held at −60, −40, −20, +20, +40, and +60 mV. (*B*) Normalized currents from (*A*) plotted on a logarithmic scale. The time scale is the same as in (*A*). The dashed lines are exponential fits to the falling phases. The decay rates were (from left to right) 1.30, 1.04, 1.10, 0.95, 1.11, and 1.14 s^{-1}. Same cilium as in Fig. 1.

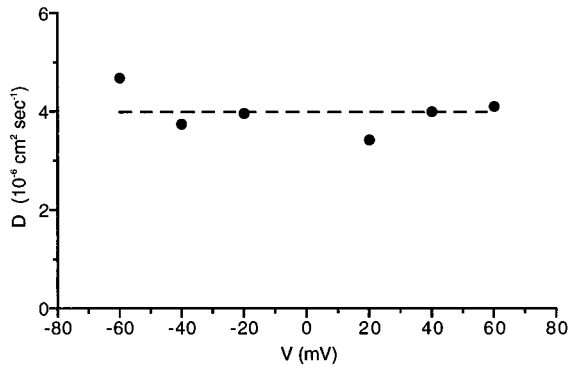

FIGURE 6 The cAMP diffusion coefficient is independent of membrane voltage. The diffusion coefficient, as calculated from the decay rates of the currents in Fig. 5, is plotted as a function of the membrane voltage. The horizontal line is a least-squares fit to the points and corresponds to a diffusion coefficient of $4 \cdot 10^{-6}\ cm^2\ s^{-1}$.

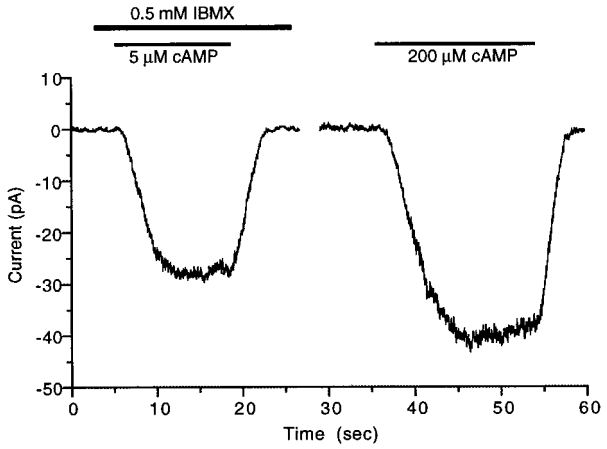

FIGURE 7 Effect of the phosphodiesterase activity on the kinetics of the cAMP-activated current. The scaling factors for the current elicited by 5 μM cAMP in the presence of 0.5 mM IBMX were 0.07 and 0.10 s^{-1} for the rising and the falling phase, respectively. For the current elicited by 200 μM cAMP in the absence of IBMX, the scaling factors were 0.008 and 1.12 s^{-1} for the rising and the falling phase, respectively. Different cilium from the one shown in Fig. 1. $L = 46$ μm.

The fit gave a diffusion coefficient value of $2.7 \pm 0.2 \cdot 10^{-6}$ cm^2 s^{-1}. This value describes the diffusion of cAMP inside the cilia at low concentrations (<5 μM).

The diffusion coefficient of several nucleotides, including AMP, in aqueous solution near physiological ionic strength has been measured to be $\sim 4 \cdot 10^{-6}$ cm^2 s^{-1} (Bowen and Martin, 1964). The close agreement between the values of the cAMP diffusion coefficient in cilia and in solution indicates that there are no significant barriers to cAMP diffusion inside the cilia. Such barriers would have been expected to reduce the value of the effective diffusion coefficient by a significant amount. In the outer segments of rod photoreceptors, baffling by the membranous disks reduces the value of the cyclic GMP (cGMP) diffusion coefficient by a factor of 6–7 (Koutalos et al., 1995a,b). In other cell types, cytoplasmic barriers and viscosity reduce the diffusion coefficient of small molecules by a factor of ~ 2 (Kushmerick and Podolsky, 1969; Caille and Hinke, 1974; Kao et al., 1993). In molluscan neurons, previous measurements have given a cAMP diffusion coefficient of $3.3 \cdot 10^{-6}$ cm^2 s^{-1} (Huang and Gillette, 1991), a value close to the one measured here for olfactory cilia. The close agreement between the values of the cAMP diffusion coefficient in cilia and in solution also suggests that there is no significant buffering at low cAMP concentrations (<5 μM). It is possible that after excision several intracellular components wash out of the cilium, perhaps including a high-affinity buffer. Nevertheless, even if such a buffer were present, it would have to be a mobile one, and thus it would not have a significant effect on the diffusion of cAMP at low cAMP concentrations.

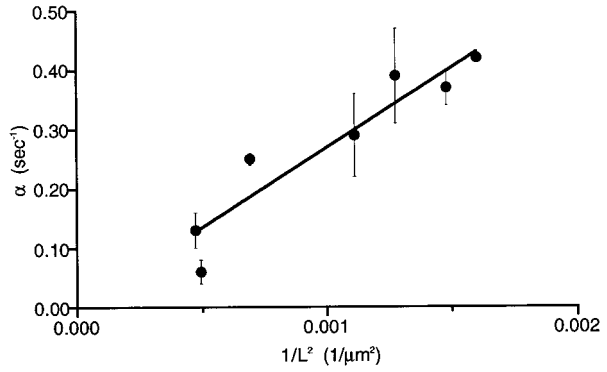

FIGURE 8 Collected results for the scaling factor α measured from different cilia and plotted as a function of the inverse square of the length of the cilium, $1/L^2$. Each point represents averaged measurements from one cilium. Error bars represent standard errors. The straight line is a least-squares fit to the data points constrained to pass through the origin. The slope of the line is $D = 2.7 \pm 0.2 \cdot 10^{-6}$ cm^2 s^{-1}.

At concentrations of cAMP higher than 5 μM, diffusion slows, as indicated by a slow secondary rise in the cAMP-activated current. Buffering was always evident in the current activated by 20 μM cAMP, but not so for the currents activated by 5 or 10 μM. In general, the slow secondary rise became more prominent at the higher cAMP concentrations. Since the maximum effect of buffering on diffusion is expected to be at concentrations close to the affinity of the sites for cAMP (see Crank, 1975, pp. 326–327), this indicates that the affinity of the binding sites for cAMP is likely to be higher than 20 μM. This affinity range suggests that the cyclic nucleotide-gated channels are unlikely to play a significant part in the buffering of cAMP.

It has been suggested (Borisy et al., 1992) that the concentration of cAMP in olfactory cilia in the absence of stimulation by odorants is ~ 1 μM. Odorant stimulation would raise the concentration to higher values. At small stimulus intensities, the produced cAMP concentration would be small, but the signal would spread along the cilium with a diffusion coefficient close to that in solution. Thus, the response to a small stimulus would be further amplified through the recruitment of additional cyclic nucleotide-gated and Cl^- channels along the cilium. As the stimulus intensity increases, cAMP would be reaching higher concentrations, but then the signal would be more restricted because of the slowing of diffusion by buffering. At the same time, the cAMP buffer would also prolong the duration of the responses elicited by stimuli of high intensities.

We thank Drs. W. J. Betz, D. Restrepo, R. Delay, and S. J. Kleene for helpful discussions and suggestions. This work was supported by NIH grant EY11351 to Y. Koutalos.

REFERENCES

Bakalyar, H. A., and R. R. Reed. 1990. Identification of a specialized adenylyl cyclase that may mediate odorant detection. *Science*. 250: 1403–1406.

Borisy, F. F., G. V. Ronnett, A. M. Cunningham, D. Juilfs, J. Beavo, and S. H. Snyder. 1992. Calcium/calmodulin-activated phosphodiesterase expressed in olfactory receptor neurons. *J. Neurosci.* 12:915–923.

Bowen, W. J., and H. L. Martin. 1964. The diffusion of adenosine triphosphate through aqueous solutions. *Arch. Biochem. Biophys.* 107:30–36.

Breer, H., I. Boekhoff, and E. Tareilus. 1990. Rapid kinetics of second messenger formation in olfactory transduction. *Nature*. 345:65–68.

Breer, H., K. Raming, and J. Krieger. 1994. Signal recognition and transduction in olfactory neurons. *Biochim. Biophys. Acta*. 1224:277–287.

Breer, H., and G. M. Shepherd. 1993. Implications of the NO/cGMP system for olfaction. *Trends Neurosci.* 16:5–9.

Caille, J. P., and J. A. M. Hinke. 1974. The volume available to diffusion in the muscle fiber. *Can. J. Physiol. Pharmacol.* 52:814–828.

Chen, T.-Y., and K.-W. Yau. 1994. Direct modulation by Ca^{2+}-calmodulin of cyclic nucleotide-activated channel of rat olfactory receptor neurons. *Nature*. 368:545–548.

Crank, J. 1975. The Mathematics of Diffusion, 2nd ed. Oxford University Press, Oxford.

Cunningham, A. M., D. K. Ryugo, A. H. Sharp, R. R. Reed, S. H. Snyder, and G. V. Ronnett. 1993. Neuronal inositol 1,4,5-trisphosphate receptor localized to the plasma membrane of olfactory cilia. *Neuroscience.* 57:339–352.

Dubin, A. E., and V. E. Dionne. 1994. Action potentials and chemosensitive conductances in the dendrites of olfactory neurons suggest new features for odor transduction. *J. Gen. Physiol.* 103:181–201.

Finn, J. T., M. E. Grunwald, and K.-W. Yau. 1996. Cyclic nucleotide-gated ion channels: an extended family with diverse functions. *Annu. Rev. Physiol.* 58:395–426.

Firestein, S., B. Darrow, and G. M. Shepherd. 1991. Activation of the sensory current in salamander olfactory receptor neurons depends on a G protein-mediated cAMP second messenger system. *Neuron*. 6:825–835.

Frings, S., J. W. Lynch, and B. Lindemann. 1992. Properties of cyclic nucleotide-gated channels mediating olfactory transduction. *J. Gen. Physiol.* 100:45–67.

Huang, R.-C., and R. Gillette. 1991. Kinetic analysis of cAMP-activated Na^+ current in the molluscan neuron: a diffusion-reaction model. *J. Gen. Physiol.* 98:835–848.

Jones, D. T., and R. R. Reed. 1989. G_{olf}: an olfactory neuron-specific G protein involved in odorant signal transduction. *Science*. 244:790–795.

Kao, H. P., J. R. Abney, and A. S. Verkman. 1993. Determinants of the translational mobility of a small solute in cell cytoplasm. *J. Cell Biol.* 120:175–184.

Kleene, S. J. 1993. Origin of the chloride current in olfactory transduction. *Neuron*. 11:123–132.

Kleene, S. J., and R. C. Gesteland. 1991a. Transmembrane currents in frog olfactory cilia. *J. Membr. Biol.* 120:75–81.

Kleene, S. J., and R. C. Gesteland. 1991b. Calcium-activated chloride conductance in frog olfactory cilia. *J. Neurosci.* 11:3624–3629.

Kleene, S. J., R. C. Gesteland, and S. H. Bryant. 1994. An electrophysiological survey of frog olfactory cilia. *J. Exp. Biol.* 195:307–328.

Koutalos, Y., R. L. Brown, J. W. Karpen, and K.-W. Yau. 1995b. Diffusion coefficient of the cyclic GMP analog, 8-(fluoresceinyl) thioguanosine 3′,5′-cyclic monophosphate in the salamander rod outer segment. *Biophys. J.* 69:2163–2167.

Koutalos, Y., K. Nakatani, and K.-W. Yau. 1995a. Cyclic GMP diffusion coefficient in rod photoreceptor outer segments. *Biophys. J.* 68:373–382.

Kramer, R. H., and S. A. Siegelbaum. 1992. Intracellular Ca^{2+} regulates the sensitivity of cyclic nucleotide-gated channels in olfactory receptor neurons. *Neuron*. 9:897–906.

Kurahashi, T., and A. Menini. 1997. Mechanism of odorant adaptation in the olfactory receptor cell. *Nature*. 385:725–729.

Kurahashi, T., and K.-W. Yau. 1993. Co-existence of cationic and chloride components in odorant-induced current of vertebrate olfactory receptor cells. *Nature*. 363:71–74.

Kushmerick, M. J., and R. J. Podolsky. 1969. Ionic mobility in muscle cells. *Science*. 166:1297–1298.

Lowe, G., and G. H. Gold. 1991. The spatial distributions of odorant sensitivity and odorant-induced currents in salamander olfactory receptor cells. *J. Physiol.* 442:147–168.

Lowe, G., and G. H. Gold. 1993. Contribution of the ciliary cyclic nucleotide-gated conductance to olfactory transduction in the salamander. *J. Physiol.* 462:175–196.

Menco, B. Ph. M. 1980. Qualitative and quantitative freeze-fracture studies on olfactory and nasal respiratory structures of frog, ox, rat, and dog. I. A general survey. *Cell Tissue Res.* 207:183–209.

Nakamura, T., and G. H. Gold. 1987. A cyclic nucleotide-gated conductance in olfactory receptor cilia. *Nature*. 325:442–444.

Nakamura, T., H.-H. Lee, H. Kobayashi, and T.-O. Satoh. 1996. Gated conductances in native and reconstituted membranes from frog olfactory cilia. *Biophys. J.* 70:813–817.

Pace, U., E. Hanski, Y. Salomon, and D. Lancet. 1985. Odorant-sensitive adenylate cyclase may mediate olfactory reception. *Nature*. 316: 255–258.

Pace, U., and D. Lancet. 1986. Olfactory GTP-binding protein: signal-transducing polypeptide of vertebrate chemosensory neurons. *Proc. Natl. Acad. Sci. USA*. 83:4947–4951.

Restrepo, D., T. Miyamoto, B. P. Bryant, and J. H. Teeter. 1990. Odor stimuli trigger influx of calcium into olfactory neurons of the channel catfish. *Science*. 249:1166–1168.

Ronnett, G. V., H. Cho, L. D. Hester, S. F. Wood, and S. H. Snyder. 1993. Odorants differentially enhance phosphoinositide turnover and adenylyl cyclase in olfactory receptor neuronal cultures. *J. Neurosci.* 13: 1751–1758.

Ronnett, G. V., and S. H. Snyder. 1992. Molecular messengers of olfaction. *Trends Neurosci.* 15:508–513.

Schild, D., and D. Restrepo. 1998. Transduction mechanisms in vertebrate olfactory receptor cells. *Physiol. Rev.* 78:429–466.

Sklar, P. B., R. R. H. Anholt, and S. H. Snyder. 1986. The odorant-sensitive adenylate cyclase of olfactory receptor cells. *J. Biol. Chem.* 261:15538–15543.

Verma, A., D. J. Hirsch, C. E. Glatt, G. V. Ronnett, and S. H. Snyder. 1993. Carbon monoxide: a putative neural messenger. *Science*. 259:381–384.

Zufall, F., S. Firestein, and G. M. Shepherd. 1994. Cyclic nucleotide-gated ion channels and sensory transduction in olfactory receptor neurons. *Annu. Rev. Biophys. Biomol. Struct.* 23:577–607.